Journal of Luminescence 288 (2025) 121540

Contents lists available at ScienceDirect

Journal of Luminescence

journal homepage: www.elsevier.com/locate/jlumin

Full Length Article

White Random Laser based on a $Ho^{3+}/Tm^{3+}/Yb^{3+}$ doped GeO_2-PbO glass

Jessica Dipold [a], Cid B. de Araújo [b], Luciana R.P. Kassab [c], Niklaus U. Wetter [a,*]

[a] Instituto de Pesquisas Energéticas e Nucleares, CNEN-IPEN, São Paulo, SP, 05508-000, Brazil
[b] Departamento de Física, Universidade Federal de Pernambuco, 50670-901, Recife, PE, Brazil
[c] Faculdade de Tecnologia de São Paulo, CEETEPS, São Paulo, SP, Brazil

ARTICLE INFO

Keywords:
Random laser
White light
Heavy-metal oxide glass
White random laser

ABSTRACT

A white Random Laser based on $Ho^{3+}/Tm^{3+}/Yb^{3+}$ doped GeO_2-PbO glass system was developed. By varying the excitation laser wavelength between 974 and 976 nm, emissions spanning blue (~480 nm), green (~547 nm) and red (~660 nm) wavelengths were obtained. The three colors emitted presented random laser behavior, evaluated by the emission intensity spectra measured by changing the excitation laser energy. White light emission was confirmed through analysis of the CIE 1931 chromaticity diagram with coordinates consistently falling within the white light region. To our knowledge, this is the first white Random Laser based on a glass doped with rare-earth ions.

1. Introduction

The original ideas of Lethokov et al. [1,2] and the seminal work by Lawandy et al. [3] activated the important research area of Random Lasers (RLs). Considerable efforts have been made by many research groups along the last three decades to accomplish random lasing operation in many material systems emitting from the ultraviolet to near-infrared as illustrated in Refs. [4–12]. Currently, research on RLs is still attracting significant attention because it enables deeper understanding of light-matter interactions, opening doors for development of new technologies and applications.

No conventional optical cavity is required for operation of RLs because they are based on the multiple scattering of light inside the gain medium, which provides the feedback for light amplification.

The absence of an optical cavity allows RLs to be integrated into arbitrary systems, enabling their use in compact devices as for example in Refs. [13,14]. Moreover, RLs can be constructed from simple materials, making them cost-effective and adaptable for use with flexible materials and disposable devices [15–19]. RLs have demonstrated good laser efficiency and show highly directional emission properties when incorporated into microfluidic devices [20,21]. A very important characteristic of RLs is the possibility to produce bright and speckle-free light which is highly wanted for applications in imaging and displays [18]. It is already well recognized that RLs are excellent alternative for various applications including fluorescence microscopy, displays and biosensors [22].

From the point of view of fundamental studies, RLs can be used as platforms to investigate many phenomena associated to complex systems including replica symmetry breaking [9,23], extreme statistical effects [9,24–27], and turbulence [9,28].

Both inorganic and organic materials have been exploited for RLs operation [11,21,29,30] although inorganic systems are more chemically and thermally stable than organic materials. In general, inorganic materials tolerate higher operating temperatures and sustained use without large degradation.

A few years ago, there were some attempts to demonstrate white Random Lasers (WRLs) by a combination of red, green, and blue (RGB) luminescent materials. In principle, by selecting one excitation wavelength to provide population inversion in a RGB system, it is possible to obtain white light emission from composite systems. Then, WRLs were demonstrated based on organic materials [31–33] and upconversion crystalline nanoparticles doped with rare-earth ions [34]. The experiments of ref. [34] were made with $NaYF_4$:Yb/Er/Tm@$NaYF_4$:Eu core-shell nanoparticles deposited on top of an Au/MoO_3 multilayer hyperbolic meta-material. The samples' fabrication in this case is much elaborated because it requires the synthesis of the upconversion nanoparticles and the fabrication of hyperbolic meta-materials to observe enhancement of the RL intensity.

We reported recently that heavy-metal oxide (HMO) glasses doped with rare-earth ions are very appropriate RLs hosts because, in comparison with many photonic glasses (such as silicates, borates, and fluorides), they present better thermal, mechanical and chemical

* Corresponding author.
E-mail address: nuwetter@ipen.br (N.U. Wetter).

https://doi.org/10.1016/j.jlumin.2025.121540
Received 10 February 2025; Received in revised form 20 August 2025; Accepted 11 September 2025
Available online 12 September 2025

durability, the possibility of fabrication in ambient atmosphere, as well as higher linear and nonlinear refractive index [35–40]. Moreover, due to their low phonons' energies (740-880 cm^{-1}) [41], HMO glasses doped with rare-earth ions present large photoluminescence. Recent investigations based on neodymium doped tellurite and germanate glass powders [10,42,43], and glass-ceramics powders [44], were successful to demonstrate the use of HMO glasses for RLs operation in the visible and near-infrared.

In the present paper, we report the first WRL based on a GeO_2-PbO glass sample doped with Tm^{3+}, Ho^{3+}, and Yb^{3+}. The excitation light wavelength was selected such that the incident optical beam could excite the trichromatic components. A WRL emitting light in a combination of blue (~480 nm), green (~547 nm) and red (~660 nm) wavelengths was obtained. In Section 2, we describe the sample fabrication and characterization. In Section 3, we describe the optical characterization of the RL emissions, the behavior of the emitted intensity as a function of the excitation laser intensity, and the analysis of the colors emitted by the samples as a function of the laser excitation intensity. In Section 4, we summarize and discuss the experimental results.

2. Materials and methods

The sample studied was produced with the well-known melt-quenching technique, using high-purity reagents (99.999 %) from Sigma-Aldrich, with the following composition (in wt.%) 59.0 PbO-41.0 GeO_2 and the incorporation of the doping species: Tm_2O_3 (0.6), Ho_2O_3 (0.65) and Yb_2O_3 (3.2). The choice of the relative oxides concentrations was made with basis on our previous photoluminescence studies to produce white light [39]. A high-purity alumina crucible (99.999 %) was employed for the melting process, which was maintained at 1200 °C for 1 h. Subsequently, the melt was quenched on a preheated brass mold and annealed at 420 °C for 1 h to reduce internal stress. Finally, the sample was cooled to room temperature.

The obtained glass sample was then grinded using an agate mortar and pestle to obtain a very fine powder, passing through a mesh with 20 μm pores. From previous works, it was noticed that for a glass powder to produce efficient RL action, the particles must be smaller than 3 μm for optimal results. Therefore, isopropyl alcohol was added to the obtained powder and left in an ultrasound bath for 3 min, then left to rest for 30 s to separate the supernatant, smaller particles, from the heavier, larger ones. The supernatant particles obtained produced a size distribution with average dimensions of 1.5 μm, as shown in a previous work using the same method described in Ref. [10]. 50 mg of the supernatant powder was mixed with 0.05 mL of isopropyl alcohol to make a paste, which was placed on a microscope slide in a 5 mm × 2.5 mm area with ~50 μm thickness and left to dry at ambient temperature.

For the RL measurements, an OPO system (OPOTEK, INC - model OPOLette) with pulse duration of 10 ns and repetition rate of 20 Hz was used as the excitation light source. The experimental setup is illustrated in Fig. 1a, where the OPO beam was focused on the sample and the luminescence was reflected with a small angle in the direction of an OceanOptics® HR2000+ Spectrometer to observe all emission wavelengths. A short-pass filter of 800 nm was used to block the pump beam and still observe the visible light emission from the sample.

The absorbance spectrum of the $Ho^{3+}/Tm^{3+}/Yb^{3+}$ doped GeO_2-PbO glass system is shown in Fig. 1b, where the $^2F_{7/2} \rightarrow {}^2F_{5/2}$ transition (980 nm for Yb^{3+}) starting from the ground state is indicated.

The frequency upconversion process that originates the spectra of Fig. 1c was discussed in detail in Refs. [38,39]. In simple terms, the excited Yb^{3+} interacts with the neighbors Ho^{3+} and Tm^{3+}, transferring energy that promotes those ions to excited states. The excited Ho^{3+} and Tm^{3+} decay, emitting the spectra shown in Fig. 1c.

The excitation (pump) wavelength varied from 974 nm up to 980 nm, to achieve emission closer to white. A comparison between emissions obtained with each excitation wavelength can be seen in Fig. 1c.

Since linewidth narrowing during laser action is not observed in glasses, because of inhomogeneous broadening of the electronic transitions [45], lasing behavior was confirmed by measuring the emission intensity per incident laser pulse energy, obtained by measuring the spectrometer intensity output. Using the Origin 2024 software we converted the measured spectra to coordinates for the CIE 1931 chromaticity diagram, which allows evaluation of how white the light emission is. The emission is considered pure white at a particular coordinate, (0.33, 0.33), but there are a set of coordinates around this point that are considered as the white light region, which were considered in the present study [46].

3. Results and discussion

3.1. emission studies

For each excitation wavelength, the emission was measured for pump laser pulses with energies between 52 and 501 μJ per pulse. The results found for the wavelengths 974 nm, 975 nm and 976 nm will be presented through the rest of the section.

The emission spectra for each excitation wavelength are shown in Fig. 2. Three main emission bands are observed: one spectral band in blue with center at ~480 nm (corresponding to Tm^{3+} transition: $^1G_4$ -$^3H_6$); one band in green at ~ 547 nm (Ho^{3+} transition: ($^5S_2$,$^5F_4$) - $^5I_8$); and another in red at ~660 nm (Tm^{3+}:$^1G_4$ -$^3F_4$ and Ho^{3+}: $^3F_5$-$^5I_8$).

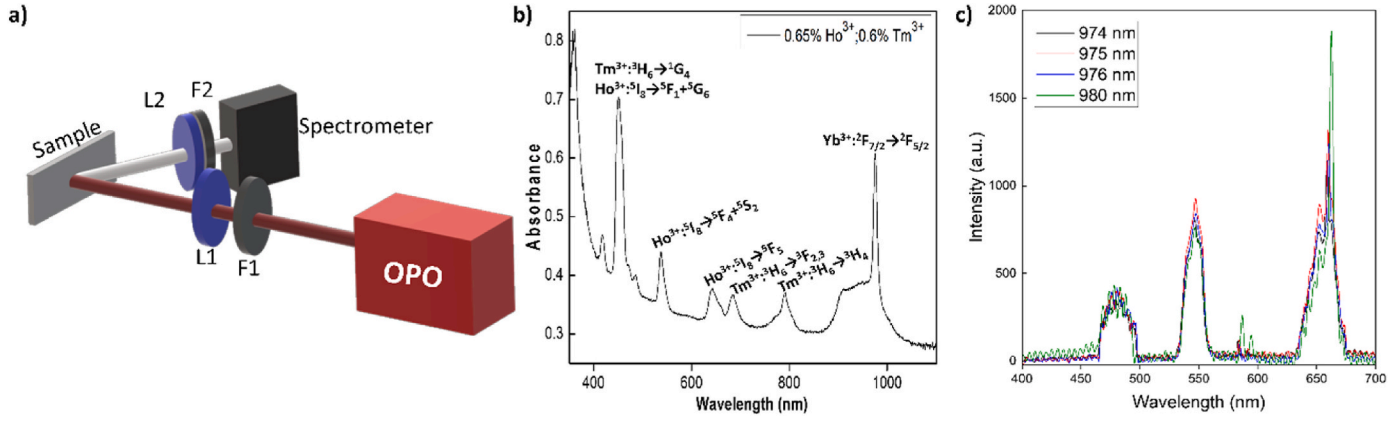

Fig. 1. a) Experimental setup. The OPO beam is focused through a 15 cm focal length lens (L1) after passing through a long-pass 900 nm filter (F1), reaching the sample. The scattered light is then collected by a telescope with 5 cm and 2.5 cm focal length lenses (L2), passing through a short-pass 800 nm filter (F2) before reaching the 50 μm diameter fiber and the HR2000+ spectrometer. b) Absorbance measurement of the studied sample (thickness: 3 mm), along with the transitions for each band; c) Measurements taken at 200 μJ excitation pulse energy for the sample for different excitation wavelengths.

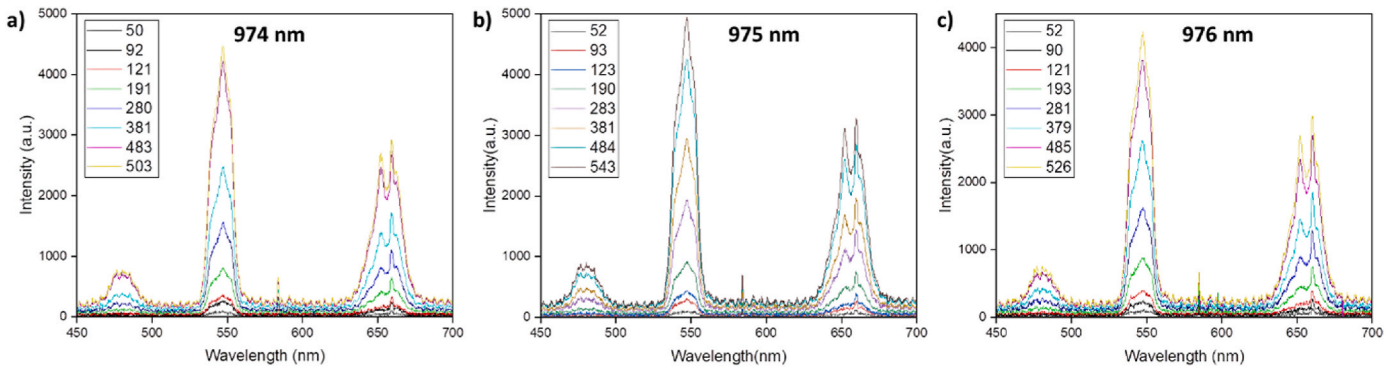

Fig. 2. Emission for a) 974 nm, b) 975 nm and c) 976 nm pump wavelength. The band located near 660 nm exhibits spikes, which is evidence of coherent feedback.

Emission bands were analyzed independently to evaluate their individual random lasing characteristics for each excitation wavelength. They were fitted one by one and integrated. The results are displayed in Fig. 3, which shows the emission intensity versus pump energy for each excitation wavelength.

From Fig. 3, it is possible to observe RL behavior for every emitted color corresponding to the three excitation wavelengths used. The most efficient emission occurs at 660 nm, where maximum intensity is reached for all excitation wavelengths, while the lowest efficiency happens for the 480 nm emission.

The thresholds for each pump wavelength are shown in Table 1. They were calculated by fitting two straight lines to the slope. The threshold is defined as the point where the two lines intersect. The smallest thresholds are present, for all emission wavelengths, with the 976 nm pump, with values between 80 μJ and 120 μJ. For the 975 nm pump, these values are larger, between 110 and 150 μJ, while for 974 nm they are between 160 and 210 μJ.

For all excitation wavelengths, the red emission at 660 nm is the one that starts lasing with the smaller pump pulse energy, while the blue emission at 480 nm requires the larger excitation pulse energy.

3.2. color analysis

As observed previously in this material [39], the bulk glass emits white photoluminescence when the pump laser operates at 980 nm, even though laser emission was not analyzed in those experiments. Here, we have already shown in the previous section that there is RL emission for three different wavelengths in red, green and blue. From these emission spectra, we verified that the effective laser color (combination of the three emission bands) is in the white light region of the CIE 1931 chromaticity diagram. The results are shown in Fig. 4 for each excitation wavelength.

A closer look shows variation of the emission color depending on the pump energy used, which is further shown in Fig. 5. Notice that for the lowest pump energies (50–60 μJ), the glass powder is emitting within the white region, with values close to the pure white coordinates. For 974 nm and low energy, the closest coordinates to pure white are (0.33, 0.36); for 975 nm, (0.32, 0.37); and for 976 nm, (0.34, 0.37). However, as the pump energy increases, the emission turns towards the green for all samples, even though at 976 nm pump wavelength the emission remains in the white light region throughout the whole range of incident energies.

For 974 nm incidence, the emission starts at CIE coordinates (0.33, 0.36) at 50 μJ pump energy. The color coordinates shift towards the green region with increasing pump power, reaching the limit between the white light region and green at 280 μJ at CIE coordinates of (0.33, 0.44). At 483 μJ pump energy it shifts further to green to coordinates (0.32, 0.44). Therefore, white random laser occurs for pump energies between 200 and 280 μJ.

For 975 nm, the emission starts at CIE coordinates (0.32, 0.37) at 52 μJ pump energy. The emission remains in the white region up to 320 μJ, presenting CIE coordinates at the limit of (0.34, 0.44). For even higher pump energies, it shifts into the green region, with (0.33, 0.44) coordinates at 543 μJ. This demonstrates white random laser between 150 and 320 μJ.

At 976 nm pump, the emission is always within the white region, varying from (0.34, 0.37) at 52 μJ pump energy up to (0.33, 0.44) at 501 μJ. This shows white random laser behavior for all pump energies between 120 and 526 μJ.

4. Conclusions

The operation of a White Random Laser was demonstrated with basis on a $Ho^{3+}/Tm^{3+}/Yb^{3+}$ doped GeO_2-PbO glass excited in the spectral region from 974 to 976 nm. Emission in three different wavelengths, blue (~480 nm), green (~547 nm) and red (~660 nm), with clear RLs

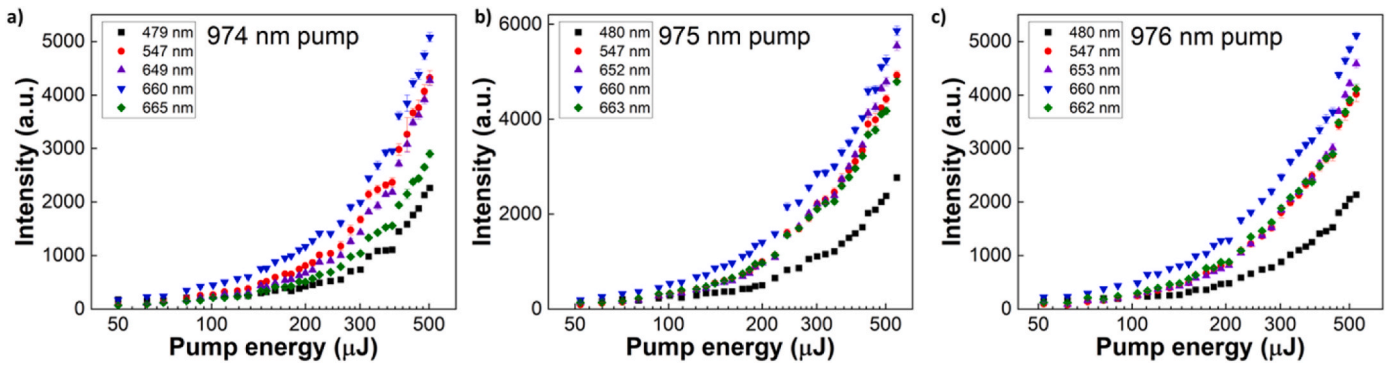

Fig. 3. Emission intensity for excitation at a) 974 nm, b) 975 nm and c) 976 nm for each emission wavelength (black squares – 480 nm, red circles – 547 nm, purple triangles – 650 nm, blue upside-down triangle – 660 nm and green diamond – 663 nm).

Table 1
Laser thresholds for each excitation and emission wavelengths.

(Pump) Excitation wavelength	Threshold for 480 nm (±10 μJ)	Threshold for 547 nm (±10 μJ)	Threshold for 650 nm (±10 μJ)	Threshold for 660 nm (±10 μJ)	Threshold for 663 nm (±10 μJ)
974 nm	210	180	200	160	170
975 nm	150	120	150	110	120
976 nm	120	90	110	80	110

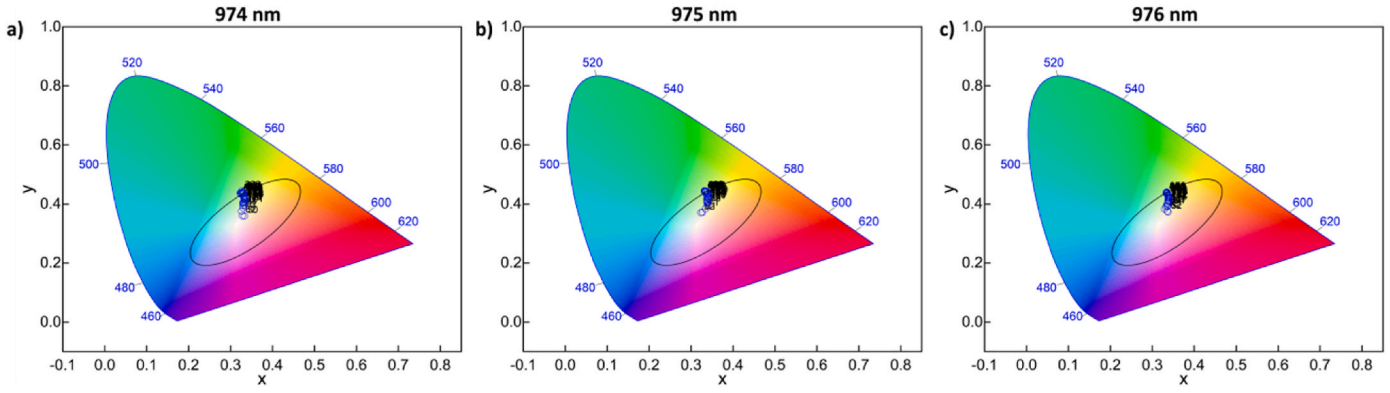

Fig. 4. Color diagram of the emitted spectra for various incident laser pulse energies with a) 974 nm, b) 975 nm and c) 976 nm excitation wavelength. The elliptical shape shows the white light region. Insets show a zoom of the studied points, with the gray area being inside the white region and the numbers the incident laser intensity.

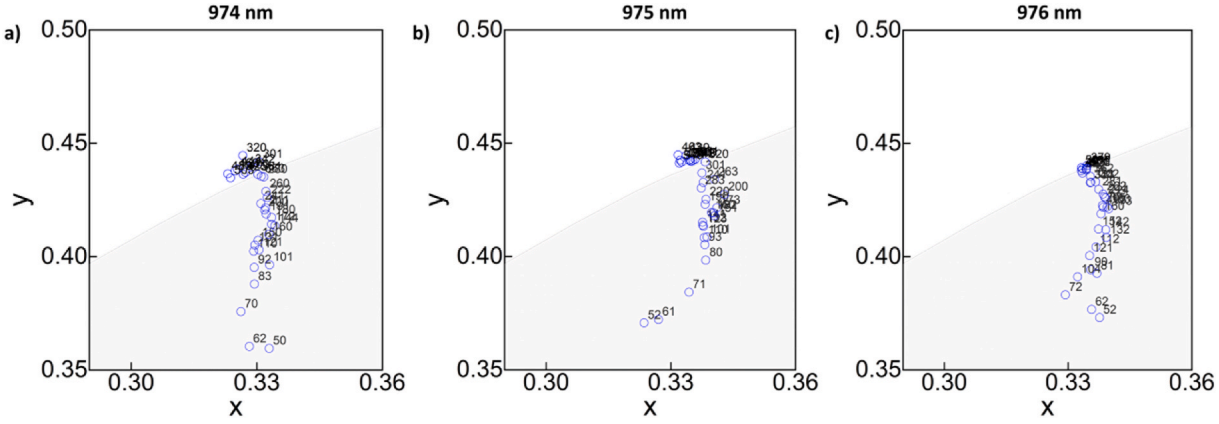

Fig. 5. Zoom of the border of the white region shown in Fig. 4 to show emission for all pump energies for a) 974 nm, b) 975 nm and c) 976 nm pump wavelengths.

thresholds was verified for each of them. The combination of the three emitted colors corresponds to white light according to the CIE 1931 chromaticity diagram. The relative concentration of the rare-earth ions is crucial to obtain the appropriate balance between the three primary colors emissions.

Different excitation wavelengths were used to verify the best output considering the emission intensity as well as location in the white light region. Considering the emitted intensities, the best results were observed for the 975 nm excitation wavelength, though it presented emission out of the white zone for energies larger than 300 μJ. For evaluation in terms of white light random laser, the pump wavelength at 976 nm presented the best result, with all pump energies leading to emission in the white light region, as well as smaller thresholds for all emission bands.

In conclusion, we demonstrated that the germanate-lead oxide glass doped with appropriate concentrations of Ho^{3+}, Tm^{3+}, and Yb^{3+} is a good material for operation of white Random Lasers due to its easy fabrication and simple tuning conditions.

CRediT authorship contribution statement

Jessica Dipold: Writing – review & editing, Writing – original draft, Methodology, Investigation, Funding acquisition, Formal analysis, Data curation. **Cid B. de Araújo:** Writing – review & editing, Writing – original draft, Methodology, Investigation, Funding acquisition, Conceptualization. **Luciana R.P. Kassab:** Writing – review & editing, Writing – original draft, Resources, Investigation, Funding acquisition, Conceptualization. **Niklaus U. Wetter:** Writing – review & editing, Writing – original draft, Supervision, Resources, Project administration, Methodology, Investigation, Funding acquisition, Formal analysis, Data curation, Conceptualization.

Declaration of competing interest

The authors declare that they have no known competing financial interests or personal relationships that could have appeared to influence the work reported in this paper.

Acknowledgments

This work was supported by IPEN-CNEN [grant IPEN/CNEN 2020.06.IPEN.33.PD], São Paulo Research Foundation (FAPESP) [grant numbers: 2019/06334-4, 2017/10765-5], the Conselho Nacional de Desenvolvimento Científico e Tecnológico (CNPq) [grant numbers: 308526/2021-0, 395745/2023-9, 406441/2023-5], the National Institute of Photonics (INCT de Fotônica) [grant: 465.763/2014], and Sisfoton project [grant: 440228/2021-2] also supported by CNPq.

Data availability

Data will be made available on request.

References

[1] R. Ambartsumyan, N. Basov, P. Kryukov, V. Letokhov, A laser with Nonresonant feedback, Soviet Physics JETP-USSR 24 (1967) 724–729.
[2] V. Letokhov, Generation of light by a scattering medium with Negative resonance Absorption, Soviet Physics JETP-USSR 26 (1968) 835–840.
[3] N. Lawandy, R. Balachandran, A.S.L. Gomes, E. Sauvain, Laser action in Strongly scattering media, Nature 368 (1994) 436–438.
[4] H. Cao, Y.G. Zhao, S.T. Ho, E.W. Seelig, Q.H. Wang, R.P.H. Chang, Random laser action in semiconductor powder, Phys. Rev. Lett. 82 (1999) 2278–2281, https://doi.org/10.1103/PhysRevLett.82.2278.
[5] H. Cao, Lasing in random media, Waves Random Media 13 (2003) R1–R39.
[6] M.A. Noginov, Solid-State Random Lasers, Springer, Berlin, 2005.
[7] A.S.L. Gomes, A.L. Moura, C.B. de Araújo, E.P. Raposo, Recent advances and applications of random lasers and random fiber lasers, Prog. Quant. Electron. 78 (2021), https://doi.org/10.1016/j.pquantelec.2021.100343.
[8] N. Padiyakkuth, S. Thomas, R. Antoine, N. Kalarikkal, Recent progress and prospects of random lasers using advanced materials, Mater. Adv. 3 (2022) 6687–6706, https://doi.org/10.1039/d2ma00221c.
[9] A.S.L. Gomes, A.L. Moura, C.B. de Araújo, E.P. Raposo (Eds.), Lévy Statistics and Spin Glass Behavior in Random Lasers, Jenny Stanford Publishing, New York, 2023.
[10] J. Dipold, C.D.S. Bordon, E.S. Magalhaes, L.R.P. Kassab, E. Jimenez-Villar, N. U. Wetter, 1337 nm emission of a Nd^{3+}-doped TZA glass random laser, Nanomaterials 13 (2023), https://doi.org/10.3390/nano13131972.
[11] J. Dipold, L.R.P. Kassab, N. Nd Wetter, YVO_4 random laser with preferential emission at 1340 nm over 1064 nm, Photonics 11 (2024), https://doi.org/10.3390/photonics11100898.
[12] R.J.R. Vieira, L. Gomes, J.R. Martinelli, N.U. Wetter, Upconversion luminescence and decay kinetics in a diode-pumped nanocrystalline Nd^{3+}:YVO4 random laser, Opt. Express 20 (2012) 12487–12497, https://doi.org/10.1364/oe.20.012487.
[13] C. Wang, C. Nieh, T. Lin, Y. Chen, Electrically driven random laser Memory, Adv. Funct. Mater. 25 (2015) 4058–4063, https://doi.org/10.1002/adfm.201500734.
[14] A. Consoli, N. Caselli, C. López, Electrically driven random lasing from a modified Fabry-Perot laser diode, Nat. Photonics 16 (2022) 219, https://doi.org/10.1038/s41566-021-00946-0.
[15] A.S.L. Gomes, D. Valente, H.P. de Oliveira, S.J.L. Ribeiro, C.B. de Araújo, Optical materials for flexible and Stretchable random lasers, Opt. Mater. X 16 (2022) 100203, https://doi.org/10.1016/j.omx.2022.100203.
[16] C.J.S. de Matos, L.D.S. Menezes, A.M. Brito-Silva, M.A.M. Gamez, A.S.L. Gomes, C. B. de Araújo, Random fiber laser, Phys. Rev. Lett. 99 (2007) 152903, https://doi.org/10.1103/PhysRevLett.99.153903.
[17] I. Viola, N. Ghofraniha, A. Zacheo, V. Arima, C. Conti, G. Gigli, Random laser emission from a paper-based device, J. Mater. Chem. C 1 (2013) 8128–8133, https://doi.org/10.1039/c3tc31860e.
[18] B. Redding, M.A. Choma, H. Cao, Speckle-free laser imaging using random laser illumination, Nat. Photonics 6 (2012) 355–359, https://doi.org/10.1038/nphoton.2012.90.
[19] A. Consoli, D.M. da Silva, N.U. Wetter, C. Lopez, Large area resonant feedback random lasers based on dye-doped biopolymer films, Opt. Express 23 (2015) 29954–29963, https://doi.org/10.1364/oe.23.029954.
[20] K.C. Jorge, M.A. Alvarado, E.G. Melo, M.N.P. Carreno, M.I. Alayo, N.U. Wetter, Directional random laser source consisting of a HC-ARROW reservoir connected to channels for spectroscopic analysis in microfluidic devices, Appl. Opt. 55 (2016) 5393–5398, https://doi.org/10.1364/ao.55.005393.
[21] N.U. Wetter, J.M. Giehl, F. Butzbach, D. Anacleto, E. Jimenez-Villar, Polydispersed powders (Nd^{3+}:YVO_4) for Ultra efficient random lasers, Part. Part. Syst. Char. 35 (2018), https://doi.org/10.1002/ppsc.201700335.
[22] E. Ignesti, F. Tommasi, L. Fini, F. Martelli, N. Azzali, S. Cavalieri, A new class of optical sensors: a random laser based device, Sci. Rep. 6 (2016), https://doi.org/10.1038/srep35225.
[23] A.S.L. Gomes, E. Raposo, A.L. Moura, S. Fewo, P. Pincheira, V. Jerez, L. Maia, C. B. de Araújo, Observation of Levy distribution and replica symmetry breaking in random lasers from a single set of measurements, Sci. Rep. 6 (2016) 27987, https://doi.org/10.1038/srep27987.
[24] B. Lima, P. Pincheira, E. Raposo, L. de S. Menezes, C.B. de Araújo, A.S.L. Gomes, R. Kashyap, Extreme-value statistics of intensities in a cw-pumped random fiber laser, Phys. Rev. 96 (2017) 013834, https://doi.org/10.1103/PhysRevA.96.013834.
[25] E. Jimenez-Villar, I.F. da Silva, V. Mestre, N.U. Wetter, C. Lopez, P.C. de Oliveira, W.M. Faustino, G.F. de Sa, Random lasing at localization transition in a colloidal Suspension (TiO_2@Silica), ACS Omega 2 (2017) 2415–2421, https://doi.org/10.1021/acsomega.7b00086.
[26] E. Jimenez-Villar, V. Mestre, P.C. de Oliveira, G.F. de Sa, Novel core-shell (TiO_2@Silica) nanoparticles for scattering medium in a random laser: higher efficiency, lower laser threshold and lower photodegradation, Nanoscale 5 (2013) 12512–12517, https://doi.org/10.1039/c3nr03603k.
[27] N. Wetter, E. Jimenez-Villar, Random laser materials: from ultrahigh efficiency to very low threshold (Anderson localization), J. Mater. Sci. Mater. Electron. 30 (2019) 16761–16773, https://doi.org/10.1007/s10854-019-01289-x.
[28] I. González, B. Lima, P. Pincheira, A. Brum, A.M. Macêdo, G. Vasconcelos, L. de S. Menezes, E. Raposo, A.S.L. Gomes, R. Kashyap, Turbulence hierarchy in a random fibre laser, Nat. Commun. 8 (2017), https://doi.org/10.1038/ncomms15731.
[29] N.U. Wetter, A.R. de Miranda, E. Pecoraro, S.J.L. Ribeiro, E. Jimenez-Villar, Dynamic random lasing in silica aerogel doped with rhodamine 6G, RSC Adv. 8 (2018) 29678–29685, https://doi.org/10.1039/c8ra04561e.
[30] C.T. Dominguez, A.A.V. Gomes, N.U. Wetter, J. Dipold, V. Mestre, W.S. Martins, E. Jimenez-Villar, Random lasing at localization induced in correlated colloidal system, Opt. Mater. 120 (2021) 111428, https://doi.org/10.1016/j.optmat.2021.111428.
[31] S. Chang, W. Liao, Y. Liao, H. Lin, H. Lin, W. Lin, S. Lin, P. Perumal, G. Haider, C. Tai, et al., A white random laser, Sci. Rep. 8 (2018), https://doi.org/10.1038/s41598-018-21228-w.
[32] A. Szukalska, A. Szukalski, M. Adaszynski, J. Mysliwiec, White lasing and white fluorescence from the Simplified two-Dyes organic system, Adv. Opt. Mater. 11 (2023), https://doi.org/10.1002/adom.202300266.
[33] J. Wang, S. Zhang, Y. Li, C. Wu, W. Zhang, H. Zhang, Z. Xie, S. Zhou, Ultra-broadband random laser and white-light emissive Carbon Dots/Crystal in-Situ Hybrids, Small 18 (2022), https://doi.org/10.1002/smll.202203152.
[34] G. Haider, H. Lin, K. Yadav, K. Shen, Y. Liao, H. Hu, P. Roy, K. Bera, K. Lin, H. Lee, et al., A highly-efficient single Segment white random laser, ACS Nano 12 (2018) 11847–11859, https://doi.org/10.1021/acsnano.8b03035.
[35] W. Dumbaugh, J. Lapp, Heavy-metal oxide glasses, J. Am. Ceram. Soc. 75 (1992) 2315–2326.
[36] L.R.P. Kassab, L.C. Courrol, A.S. Morais, C.M.S.P. Mendes, S.H. Tatumi, N. U. Wetter, L. Gomes, V.L.R. Salvador, Spectroscopic properties of lead fluoroborate and heavy metal oxide glasses doped with Yb3+, J. Non-Cryst. Solids 304 (2002) 233–237, https://doi.org/10.1016/S0022-3093(02)01028-1.
[37] P. Nachimuthu, M. Vithal, R. Jagannathan, Absorption and emission spectral properties of Pr^{3+} , Nd^{3+} , and Eu^{3+} ions in heavy-metal oxide glasses, J. Am. Ceram. Soc. 83 (2000) 597–604.
[38] M. Camilo, E. Silva, T. de Assumpçao, L. Kassab, C.B. de Araújo, White light generation in Tm^{3+}/Ho^{3+}/Yb^{3+} doped PbO-GeO_2 glasses excited at 980 nm, J. Appl. Phys. 114 (2013) 163515, https://doi.org/10.1063/1.4827863.
[39] M. Camilo, E. Silva, L. Kassab, J. Garcia, C.B. de Araújo, White light generation controlled by changing the concentration of silver nanoparticles hosted by Ho^{3+}/Tm^{3+}/Yb^{3+} doped GeO_2-PbO glasses, J. Alloys Compd. 644 (2015) 155–158, https://doi.org/10.1016/j.jallcom.2015.04.108.
[40] T. de Assumpçao, L. Kassab, A. Gomes, C.B. de Araújo, N. Wetter, Influence of the heat treatment on the nucleation of silver nanoparticles in Tm^{3+} doped PbO-GeO_2 glasses, Appl. Phys. B Laser Opt. 103 (2011) 165–169, https://doi.org/10.1007/s00340-010-4258-5.
[41] A. Jha, B. Richards, G. Jose, T. Teddy-Fernandez, P. Joshi, X. Jiang, J. Lousteau, Rare-earth ion doped TeO_2 and GeO_2 glasses as laser materials, Prog. Mater. Sci. 57 (2012) 1426–1491, https://doi.org/10.1016/j.pmatsci.2012.04.003.
[42] J.G. Câmara, D. da Silva, L.R.P. Kassab, C.B. de Araújo, Random laser emission from neodymium doped zinc tellurite glass-powder presenting luminescence concentration quenching, J. Lumin. 233 (2021) 117936, https://doi.org/10.1016/j.jlumin.2021.117936.
[43] J. Câmara, D. da Silva, L. Kassab, C.B. de Araújo, Random laser emission from neodymium doped alumina lead-germanate glass powder, Appl. Opt. 62 (2023) C59–C63, https://doi.org/10.1364/AO.476767.
[44] J. Câmara, D. da Silva, L. Kassab, G. Palacios, C.B. de Araújo, Upconversion random lasing in Er3+/Yb3+co-doped germanate-lead-magnesium glass-ceramics, Opt. Mater. 157 (2024) 116387, https://doi.org/10.1016/j.optmat.2024.116387.
[45] M. Yamane, Y. Asahara, Glasses for Photonics, Cambridge University Press, Cambridge, 2000.
[46] D. Anwar, A. Srivastava, Constellation design for single Photodetector based CSK with Probabilistic shaping and white color balance, IEEE Access 8 (2020) 159609–159621, https://doi.org/10.1109/ACCESS.2020.3020403.